To appear in *International Journal of Numerical Methods in Fluids* in 1997.

Stability analysis of numerical interface conditions in fluid-structure thermal analysis

M. B. Giles
Oxford University Computing Laboratory
Numerical Analysis Group

This paper analyses the numerical stability of coupling procedures in modelling the thermal diffusion in a solid and fluid with continuity of temperature and heat flux at the interface. A simple one-dimensional model is employed with uniform material properties and grid density in each domain. A number of different explicit and implicit algorithms are considered for both the interior equations and the boundary conditions. The analysis shows that, in general, these are stable provided Dirichlet boundary conditions are imposed on the fluid and Neumann boundary conditions are imposed on the solid; in each case, the imposed values are obtained from the other domain.

Oxford University Computing Laboratory
Numerical Analysis Group
Wolfson Building
Parks Road
Oxford, England OX1 3QD

April, 1997

1 Introduction

This analysis is motivated by interest in numerical procedures for coupling separate computations of thermal diffusion in a solid and a fluid. A typical example application is the computation of heat transfer to a blade in a gas turbine. The surrounding air in a high pressure turbine is on average at a much higher temperature and therefore there is a significant heat flux from the fluid into the turbine blade. In steady-state, this is matched by a corresponding heat transfer from the blade to relatively cold air flowing through internal cooling passages.

One approach to the numerical approximation of the above situation would be the use of a single consistent, fully-coupled discretisation modelling both the solid and the fluid, plus the boundary conditions at the interfaces [9]. However, for the solid it is the scalar unsteady parabolic p.d.e. which describes the thermal diffusion, while for the fluid the appropriate equations are the Navier-Stokes equations, with suitable turbulence modelling. Therefore, the production of a single fully-coupled code for the combined diffusion application can be as much work as writing the individual programs for the separate solid and fluid applications.

Since there are often existing codes which accurately and efficiently solve these individual problems, a more practical approach in many circumstances is to use these together to analyse coupled problems [1, 4, 8, 7, 3, 2]. Both CFD codes and thermal analysis codes usually have the capability to specify either the temperature or the heat flux at boundaries. A natural choice therefore for coupling these codes is to specify the surface temperature at the interface in one code, taking the value from the other code, and specify the boundary heat flux in the second code, taking its value from the first code [1, 4]. A concern is whether there is any possibility that this coupling procedure will introduce a numerical instability which does not exist for the uncoupled problems. This is the issue that is addressed in this study.

The general theory for the analysis of numerical interface or boundary condition instabilities is well-established [6, 11] but can be very complicated to apply in practice. In 2D and 3D computations of engineering interest, one class of error modes which might be unstable are those whose variation is purely in the direction normal to the interface between the solid and fluid. The finite difference or finite volume equations for this class of error modes reduce to being one-dimensional, and therefore in this paper we simplify the analysis for this diffusion problem by restricting attention to a simple 1D model problem with a uniform grid on either side of the interface. Since there is no velocity component normal to the solid boundary in 2D and 3D flows, it is appropriate in the 1D model problem to omit any convection term. Stability for this 1D model problem is a necessary condition for the stability of the real 2D and 3D computations. It may, or may not, be a sufficient condition for stability but understanding the nature of possible 1D instabilities clearly gives insight into the potential instabilities in 2D and 3D computations.

2 Analytic problem

The parabolic p.d.e. describing unsteady thermal diffusion is

$$c\frac{\partial T}{\partial t} = -\frac{\partial q}{\partial x}, \qquad q = -k\frac{\partial T}{\partial x} \tag{2.1}$$

Here $T(x,t)$ is the temperature, $q(x,t)$ is the heat flux, $c(x)$ is the heat capacity and $k(x)$ is the conductivity. These equations are valid for arbitrary, piecewise continuous positive functions $c(x), k(x)$. The finite volume algorithms to be analysed are all based on the integral version of this equation,

$$\frac{\mathrm{d}}{\mathrm{d}t}\int_{x_1}^{x_2} cT\mathrm{d}x = -[q]_{x_1}^{x_2}. \tag{2.2}$$

At any interface at which c and/or k are discontinuous, the equations are augmented by the requirement that T and q must be continuous.

The boundary conditions as $x \to \pm\infty$ are that the temperature asymptotes to a constant value, $T_{\pm\infty}$, and so the heat flux tends to zero.

Defining

$$T_{max}(t) = \max_x T(x,t), \qquad T_{min}(t) = \min_x T(x,t), \tag{2.3}$$

an important property of solutions of the unsteady diffusion equation is that for any non-uniform initial conditions $T(x,0)$ and for all $t>0$,

$$\frac{\mathrm{d}T_{max}}{\mathrm{d}t} \leq 0, \qquad \frac{\mathrm{d}T_{min}}{\mathrm{d}t} \geq 0. \tag{2.4}$$

Furthermore, if $T_{-\infty} = T_{+\infty}$ then $T_{min}(t) \to T_{max}(t)$ as $t \to \infty$. The behaviour of the maximum and minimum temperature will be important in defining the numerical stability of the coupled system.

Although the above theory is given for general $c(x), k(x)$, in this paper we will now restrict attention to a single interface at $x=0$ with c and k having uniform values c_-, k_- for $x<0$, and c_+, k_+ for $x>0$.

3 Fully-coupled discretisation

In this section we examine the stability of fully-coupled discretisations of the model problem. The theory for this is well established since it is simply a special case of the more general problem of the discretisation of a parabolic p.d.e. with spatially varying diffusivity [5, 10]. There are several reasons for doing this analysis even though it is believed that the fully-coupled approach is not the most practical approach to real coupled applications. The first is to show that in a good fully-coupled discretisation there are no instabilities associated with the interface treatment, that stability of the discretisation on the uniform mesh on either side of the interface is a necessary and sufficient for stability of the fully-coupled discretisation. The second is to have a benchmark against which to compare the 'weakly-coupled' discretisations in the next section. These will be shown to have interface instabilities under certain conditions, and it is informative to see how these are related to differences in the interface treatment relative to the fully-coupled discretisation.

Using a computational grid with uniform spacing Δx_- for $x<0$ and uniform spacing Δx_+ for $x>0$, the location of grid nodes is given by

$$x_j = \begin{cases} j\,\Delta x_-, & j \le 0 \\ j\,\Delta x_+, & j \ge 0 \end{cases} \tag{3.1}$$

Associated with each grid node is the discrete temperature variable T_j^n which is to approximate the analytic solution $T(x,t)$ at $x=x_j$, $t=n\Delta t$.

3.1 An explicit algorithm

Using forward Euler time differencing and conservative spatial differencing based on the integral form of the unsteady diffusion equation on the interval $x_{j-\frac{1}{2}} \le x \le x_{j+\frac{1}{2}}$ gives the following explicit algorithm,

$$C_j\,(T_j^{n+1} - T_j^n) = -(q^n_{j+\frac{1}{2}} - q^n_{j-\frac{1}{2}}), \qquad q^n_{j+\frac{1}{2}} = -K_{j+\frac{1}{2}}(T^n_{j+1} - T^n_j) \tag{3.2}$$

where

$$C_j = \begin{cases} \dfrac{c_-\Delta x_-}{\Delta t}, & j<0 \\ \frac{1}{2}\left(\dfrac{c_-\Delta x_-}{\Delta t} + \dfrac{c_+\Delta x_+}{\Delta t}\right), & j=0 \\ \dfrac{c_+\Delta x_+}{\Delta t}, & j>0 \end{cases} \tag{3.3}$$

and

$$K_{j+\frac{1}{2}} = \begin{cases} \dfrac{k_-}{\Delta x_-}, & j+\frac{1}{2}<0 \\ \dfrac{k_+}{\Delta x_+}, & j+\frac{1}{2}>0 \end{cases} \tag{3.4}$$

Note that the equation for $j=0$ involves the conductivity and heat capacity on both sides of the interface. In particular, $\Delta t\, C_0$ is the heat capacity of the whole finite volume computational cell extending from $x_{-\frac{1}{2}}$ to $x_{+\frac{1}{2}}$.

For $j \neq 0$, the difference equation reduces to

$$T_j^{n+1} = T_j^n + d_\pm \left(T_{j+1}^n - 2T_j^n + T_{j-1}^n\right) \tag{3.5}$$

where

$$d_\pm = \frac{k_\pm \Delta t}{c_\pm \Delta x_\pm^2}. \tag{3.6}$$

Standard Fourier stability analysis on either side of the interface show that a discrete Fourier mode is stable provided $d\pm \leq \frac{1}{2}$.

We will now prove that if the requirements of Fourier stability are satisfied on each side of the interface, then the fully-coupled discretisation is stable in the sense that

$$T_{max}^{n+1} \leq T_{max}^n, \qquad T_{min}^{n+1} \geq T_{min}^n, \tag{3.7}$$

where

$$T_{max}^n \equiv \max_j T_j^n, \qquad T_{min}^n \equiv \min_j T_j^n. \tag{3.8}$$

We begin by noting that if $d_\pm \leq \frac{1}{2}$ then for any positive value r

$$d_- + rd_+ \leq \tfrac{1}{2}(1+r) \implies \frac{d_- + rd_+}{1+r} \leq \tfrac{1}{2}. \tag{3.9}$$

We will use this result with r defined as the ratio of the heat capacities of the computational cells on either side of the interface,

$$r = \frac{c_+ \Delta x_+}{c_- \Delta x_-}. \tag{3.10}$$

The next step is to re-write the full difference equation as

$$T_j^{n+1} = (1 - a_j - b_j)\, T_j^n + a_j T_{j+1}^n + b_j T_{j-1}^n \tag{3.11}$$

where

$$\begin{aligned} a_j = b_j = d_-, \qquad & j < 0 \\ a_0 = \frac{2d_-}{1+r}, \qquad b_0 = \frac{2rd_+}{1+r}, & \\ a_j = b_j = d_+, \qquad & j > 0 \end{aligned} \tag{3.12}$$

$0 < d_\pm \leq \frac{1}{2}$ so for all j, a_j, b_j and $1 - a_j - b_j$ are positive quantities and thus T_j^{n+1} is a positive weighted average of $T_{j+1}^n, T_j^n, T_{j-1}^n$. Hence,

$$T_{min}^n \leq \min(T_{j+1}^n, T_j^n, T_{j-1}^n) \leq T_j^{n+1} \leq \max(T_{j+1}^n, T_j^n, T_{j-1}^n) \leq T_{max}^n \tag{3.13}$$

This is true for all j, and so taking the maximum over all j, and the minimum over all j, gives the desired result, Equation (3.7).

3.2 An implicit algorithm

Replacing the forward Euler time differencing with backward Euler time differencing gives the following implicit algorithm.

$$C_j\,(T_j^{n+1}-T_j^n) = -(q_{j+\frac{1}{2}}^{n+1}-q_{j-\frac{1}{2}}^{n+1}) \qquad q_{j+\frac{1}{2}}^{n+1} = -K_{j+\frac{1}{2}}(T_{j+1}^{n+1}-T_j^{n+1}), \tag{3.14}$$

with $C_j, K_{j+\frac{1}{2}}$ as defined before. Fourier stability analysis of the discretisation on either side of the interface shows it to be unconditionally stable.

The fully-coupled discretisation is also unconditionally stable in the same sense as before. To prove this, the difference equation is re-written as

$$T_j^{n+1} = (1-a_j-b_j)\,T_j^n \;+\; a_j T_{j+1}^{n+1} \;+\; b_j T_{j-1}^{n+1}, \tag{3.15}$$

where

$$\begin{aligned} a_j &= \frac{K_{j+\frac{1}{2}}}{K_{j+\frac{1}{2}}+K_{j-\frac{1}{2}}+C_j}, \\ b_j &= \frac{K_{j-\frac{1}{2}}}{K_{j+\frac{1}{2}}+K_{j-\frac{1}{2}}+C_j}, \\ 1-a_j-b_j &= \frac{C_j}{K_{j+\frac{1}{2}}+K_{j-\frac{1}{2}}+C_j}. \end{aligned} \tag{3.16}$$

It is clear that a_j, b_j and $1-a_j-b_j$ are positive quantities, for all j. We now choose J such that $T_J^{n+1} = T_{max}^{n+1}$. Subtracting T_{max}^{n+1} from both sides of the difference equation gives

$$(1-a_J-b_J)(T_J^n - T_{max}^{n+1}) + a_J(T_{J+1}^{n+1} - T_{max}^{n+1}) + b_J(T_{J-1}^{n+1} - T_{max}^{n+1}) = 0. \tag{3.17}$$

Because $T_{J-1}^{n+1}, T_{J+1}^{n+1} \leq T_{max}^{n+1}$ and $a_J, b_J, 1-a_J-b_J$ are all positive, either $T_J^n > T_{max}^{n+1}$ or $T_J^n = T_{J+1}^{n+1} = T_{J+1}^{n+1} = T_{max}^{n+1}$. In the first case, we immediately get the result that $T_{max}^n > T_{max}^{n+1}$. In the second case, we can repeat the argument with $j = J \pm 1$. By further repetition if necessary, we conclude that either $T_{max}^n > T_{max}^{n+1}$ or $T_j^n = T_j^{n+1} = T_{max}^{n+1}$, for all j, in which case $T_{max}^n = T_{max}^{n+1}$.

Exactly the same argument can be used to prove that $T_{min}^n \leq T_{min}^{n+1}$ with equality occurring only in the trivial case in which T_j^n is constant.

4 Loosely-coupled discretisation

In the loosely-coupled discretisation, each half of the domain is solved separately with boundary conditions containing information from the other. The natural boundary conditions for a diffusion problem are either Dirichlet (the specification of the boundary temperature) or Neumann (the specification of the boundary heat flux). Therefore we will consider a loosely-coupled procedure in which the calculation for $x \geq 0$ uses Dirichlet data obtained from the solution for $x \leq 0$, while the calculation for $x \leq 0$ uses Neumann data obtained from the solution for $x \geq 0$.

4.1 An explicit algorithm

Given existing solutions at time level n in both halves of the domain, the simplest and most natural explicit numerical algorithm for determining T_j^{n+1} for $j \leq 0$ is

$$\begin{aligned} \frac{c_- \Delta x_-}{\Delta t}\left(T_j^{n+1} - T_j^n\right) &= \frac{k_-}{\Delta x_-}\left(T_{j+1}^n - 2T_j^n + T_{j-1}^n\right), \quad j < 0 \\ \frac{c_- \Delta x_-}{2\Delta t}\left(T_0^{n+1} - T_0^n\right) &= -q_w - \frac{k_-}{\Delta x_-}\left(T_0^n - T_{-1}^n\right), \end{aligned} \tag{4.1}$$

where q_w is the heat flux specified as the interface boundary condition. Using a finite volume derivation, the equations for $j < 0$ correspond to the control volume $[x_{j-\frac{1}{2}}, x_{j+\frac{1}{2}}]$ of width Δx_-, whereas the equation for $j = 0$ corresponds to the control volume $[x_{-\frac{1}{2}}, 0]$ of width $\frac{1}{2}\Delta x_-$.

The simplest consistent equation for determining the heat flux at the interface from the data in $j \geq 0$ is

$$q_w = -\frac{k_+}{\Delta x_+}\left(T_1^n - T_0^n\right). \tag{4.2}$$

This one-sided approximation to the temperature gradient at the surface is only first order accurate during unsteady transients. However, it is typical of the numerical methods used for practical computations [8, 7].

The corresponding explicit numerical algorithm for simultaneously determining T_j^{n+1} for $j > 0$ is

$$\frac{c_+ \Delta x_+}{\Delta t}\left(T_j^{n+1} - T_j^n\right) = \frac{k_+}{\Delta x_+}\left(T_{j+1}^n - 2T_j^n + T_{j-1}^n\right). \tag{4.3}$$

The equation for $j = 1$ requires the variable T_0^n and this is set by the Dirichlet boundary condition

$$T_0^n = T_w, \tag{4.4}$$

where T_w is the interface temperature. The obvious value for this is simply T_0^n from the computation for $j \leq 0$.

To summarise the communication between the two calculations for $j \leq 0$ and $j \geq 0$, at each timestep there is an exchange of data, with the program or subroutine performing the calculation for $j \leq 0$ supplying the value of T_w to the other program or subroutine performing the calculation for $j \geq 0$, while the latter sends q_w to the former. It is then possible that the computations for the two halves could proceed in parallel (perhaps using separate processes on separate workstations) until they again exchange data before the next timestep.

By comparing Equations (4.1,4.3) with Equation (3.2), it can be seen that the only difference is the omission of the term

$$\frac{c_+ \Delta x_+}{2\Delta t}$$

in the equation for $j = 0$. If $c_+\Delta x_+ \ll c_-\Delta x_-$, then this omitted term is negligible compared to the retained term

$$\frac{c_- \Delta x_-}{2\Delta t}$$

and so it seems likely that no instability will be introduced by its omission. On the other hand, if $c_+\Delta x_+ \gg c_-\Delta x_-$, then the omitted term may be very significant. This indicates very simply that a key parameter in the following analysis will be the variable r, defined earlier in Equation (3.10) as the ratio of these two quantities.

For the purposes of analysis it is more convenient to consolidate and simplify the equations into the following form,

$$\begin{aligned} T_j^{n+1} &= T_j^n + d_- \left(T_{j+1}^n - 2T_j^n + T_{j-1}^n\right), \qquad j < 0 \\ T_0^{n+1} &= T_0^n - 2d_- \left(T_0^n - T_{-1}^n\right) + 2rd_+ \left(T_1^n - T_0^n\right), \\ T_j^{n+1} &= T_j^n + d_+ \left(T_{j+1}^n - 2T_j^n + T_{j-1}^n\right), \qquad j > 0 \end{aligned} \tag{4.5}$$

where $d_\pm$ and r are as defined previously.

In applying the stability theory of Godunov and Ryabenkii [6, 11], the task is to investigate the existence of separable normal modes of the form

$$T_j^n = z^n f_j. \tag{4.6}$$

The discretisation is unstable if the difference equation admits such solutions which satisfy the far-field boundary conditions, $f_j \to 0$ as $j \to \pm\infty$, and have $|z| > 1$, giving exponential growth in time. The form of the solution is very similar to the assumed Fourier modes, except that the amplitude of the spatial oscillation decays exponentially with $|j|$ away from the interface.

For this application the normal mode must be of the form

$$T_j^n = \begin{cases} z^n \kappa_-^j, & j \le 0 \\ z^n \kappa_+^j, & j \ge 0 \end{cases} . \tag{4.7}$$

The difference equations, Equation (4.5) are satisfied provided the three variables z, κ_-, κ_+ satisfy the following equations.

$$
\begin{aligned}
z &= 1 + d_-(\kappa_- - 2 + \kappa_-^{-1}) \\
z &= 1 + 2d_-(\kappa_-^{-1} - 1) + 2rd_+(\kappa_+ - 1) \\
z &= 1 + d_+(\kappa_+ - 2 + \kappa_+^{-1})
\end{aligned}
\tag{4.8}
$$

Solving the first of these equations to obtain κ_-^{-1} gives

$$
\kappa_-^{-1} = 1 - \frac{1-z}{2d_-}\left(1 \pm \sqrt{1 - \frac{4d_-}{1-z}}\right). \tag{4.9}
$$

To satisfy the far-field boundary conditions as $j \to -\infty$ it is necessary to choose the negative square root when the argument is real and positive. When it is complex, the choice of root is defined by the requirement that $|\kappa_-^{-1}| < 1$.

Similarly, solving the third of the equations gives

$$
\kappa_+ = 1 - \frac{1-z}{2d_+}\left(1 - \sqrt{1 - \frac{4d_+}{1-z}}\right). \tag{4.10}
$$

Substituting these into the second equation gives the following nonlinear equation for z.

$$
\sqrt{1 - \frac{4d_-}{1-z}} \quad - \quad r\left(1 - \sqrt{1 - \frac{4d_+}{1-z}}\right) = 0 \tag{4.11}
$$

There is no simple closed form solution to this, giving z as an explicit function of the parameters d_-, d_+, r. Instead, we consider asymptotic solutions under different assumptions.

When $d_-, d_+ \ll 1$, the square root terms can be expanded to give the following approximate equation and solution.

$$
1 - \frac{2d_-}{1-z} - \frac{2rd_+}{1-z} \approx 0, \quad \Longrightarrow \quad z \approx 1 - 2d_- - 2rd_+. \tag{4.12}
$$

The requirement for stability is $|z| < 1$. The solution $z(r)$ lies inside $|z| = 1$ for sufficiently small values of r, but then crosses it at $z = -1$ when $r = \frac{1}{d_+}$. Thus for $d_-, d_+ \ll 1$ the stability requirement is $r < \frac{1}{d_+}$.

Expanding the analysis to consider arbitrary values for d_-, d_+, we begin by considering the asymptotic behaviour when $r \ll 1$ and $r \gg 1$.

When $r \ll 1$, the second term in Equation (4.11) is relatively small, and the approximate solution is

$$
\sqrt{1 - \frac{4d_-}{1-z}} \approx 0, \quad \Longrightarrow \quad z \approx 1 - 4d_-. \tag{4.13}
$$

Since d_- must satisfy $0 < d_- \leq \frac{1}{2}$ for the discretisation to be stable according to Fourier stability analysis, it follows that $|z| \leq 1$. Thus, there is no coupled instability when $r \ll 1$.

When $r \gg 1$, the first term in Equation (4.11) is relatively small, and so to a first approximation the solution is

$$1 - \sqrt{1 - \frac{4d_+}{1-z}} \approx 0, \quad \Longrightarrow \quad \frac{4d_+}{1-z} \approx 0 \quad \Longrightarrow \quad |z| \gg 1. \tag{4.14}$$

To get a more accurate approximate solution, the first term is approximated using $|z| \gg 1$ to obtain

$$1 - \sqrt{1 - \frac{4d_+}{1-z}} \approx -\frac{1}{r} \quad \Longrightarrow \quad \frac{4d_+}{1-z} \approx \frac{2}{r} \quad \Longrightarrow \quad z \approx 1 - 2rd_+. \tag{4.15}$$

Thus for fixed d_+ and sufficiently large r, there is an instability with z being large, real and negative. The corresponding values of κ_-^{-1} and κ_+ will be small, real and negative, so the instability will appear as a 'sawtooth' oscillation mode, both spatially and in time, with an amplitude which decays exponentially away from the interface, but grows exponentially in time.

Since the loosely coupled system is stable for $r \ll 1$ and unstable for $r \gg 1$ the remaining question is the value of r at which the instability begins. This corresponds to the lowest positive real value of r for which $|z| = 1$. Because of the requirement that r is real, it can be shown from Equation (4.11) that this again requires $z = -1$, in which case

$$r = \frac{\sqrt{1-2d_-}}{1-\sqrt{1-2d_+}} \tag{4.16}$$

Thus the condition for stability is

$$r < \frac{\sqrt{1-2d_-}}{1-\sqrt{1-2d_+}} \tag{4.17}$$

A typical calculation with a timestep close to the Fourier stability limit might have $d_- = d_+ = \frac{3}{8}$, for which the coupled stability limit is $r < 1$. The key to obtaining stability in practical computations is the correct choice of which half of the domain uses the Dirichlet boundary conditions and which half uses the Neumann boundary conditions. The usual practice for the coupled blade/air computations discussed in the Introduction is to use Neumann boundary conditions for the solid computation, and Dirichlet boundary conditions for the fluid computation. For this choice, the corresponding value of r is given by

$$r = \frac{c_{\text{fluid}} \Delta x_{\text{fluid}}}{c_{\text{solid}} \Delta x_{\text{solid}}}. \tag{4.18}$$

Given typical values for the parameters involved, r is usually very small and so this is stable.

If, on the other hand, one were to use Dirichlet boundary conditions for the solid computation and Neumann boundary conditions for the fluid computation, then the appropriate value for r would be the inverse of the above quantity, which would be very large. In this case the coupled calculation would be unstable unless one used an extremely small timestep. Using the approximate solution for $r \gg 1$ in Equation (4.15), the timestep stability limit is given by

$$d_+ \leq \frac{1}{r}, \tag{4.19}$$

so stability of the coupled system would require the use of a timestep very much smaller than that needed for Fourier stability.

This analysis is supported by the numerical results presented in Figures 1 and 2. The computations use the finite domain $-2000 \leq j \leq 2000$, initial conditions $T_j^0 = -1$ for $j < 0$ and $T_j^0 = 1$ for $j \geq 0$ and boundary conditions $T^n_{-2000} = -1, T^n_{2000} = 1$. In addition, all of the computations use $d_- = d_+ = \frac{3}{8}$ for which the analysis above predicts the coupled system to be stable only for $r < 1$.

Figure 1 shows two sets of results with T_j^n plotted for the first 10 iterations in each case. In a), $r = \frac{1}{2}$ and the solution is clearly stable, with an initial transient at the interface decaying very quickly, while in b), $r = 2$ and the solution is very unstable. Figure 2 shows another two sets of results with T_j^n plotted every 25 iterations. In a), $r = 0.99$ and the solution appears to be stable, although with the interface transient decaying more slowly in this case, while in b), $r = 1.01$ and the solution is clearly unstable.

4.2 A hybrid algorithm

The next algorithm to consider is a hybrid one, in which the computation is unaltered for $j > 0$, but the algorithm for $j \leq 0$ is replaced by the corresponding implicit method based on a backward Euler time discretisation.

$$\begin{aligned} \frac{c_-\Delta x_-}{\Delta t}(T_j^{n+1} - T_j^n) &= \frac{k_-}{\Delta x_-}(T_{j+1}^{n+1} - 2T_j^{n+1} + T_{j-1}^{n+1}), \quad j < 0 \\ \frac{c_-\Delta x_-}{2\Delta t}(T_0^{n+1} - T_0^n) &= -q_w - \frac{k_-}{\Delta x_-}(T_0^{n+1} - T_{-1}^{n+1}). \end{aligned} \tag{4.20}$$

The boundary heat flux q_w is again defined explicitly by

$$q_w = -\frac{k_+}{\Delta x_+}(T_1^n - T_0^n). \tag{4.21}$$

The difference equations for $j > 0$ are unchanged, as is the communication of data between the calculations for $j \leq 0$ and $j > 0$.

The consolidated, simplified form of the equations is

$$\begin{aligned} T_j^{n+1} &= T_j^n + d_- \left(T_{j+1}^{n+1} - 2T_j^{n+1} + T_{j-1}^{n+1}\right), \qquad j < 0 \\ T_0^{n+1} &= T_0^n - 2d_- \left(T_0^{n+1} - T_{-1}^{n+1}\right) + 2rd_+ \left(T_1^n - T_0^n\right), \\ T_j^{n+1} &= T_j^n + d_+ \left(T_{j+1}^n - 2T_j^n + T_{j-1}^n\right), \qquad j > 0 \end{aligned} \tag{4.22}$$

and the normal mode is again of the form

$$T_j^n = \begin{cases} z^n \kappa_-^j, & j \le 0 \\ z^n \kappa_+^j, & j \ge 0 \end{cases}. \tag{4.23}$$

The difference equations, Equation (4.22) are satisfied provided the three variables z, κ_-, κ_+ satisfy the following equations.

$$\begin{aligned} 1 &= z^{-1} + d_-(\kappa_- - 2 + \kappa_-^{-1}) \\ 1 &= z^{-1} + 2d_-(\kappa_-^{-1} - 1) + 2rd_+ z^{-1}(\kappa_+ - 1) \\ z &= 1 + d_+(\kappa_+ - 2 + \kappa_+^{-1}) \end{aligned} \tag{4.24}$$

The third of these equations requires that κ_+ depends on z in exactly the same way as for the purely explicit algorithm. Solving the first of these equations subject to the far-field boundary conditions gives

$$\kappa_-^{-1} = 1 + \frac{1 - z^{-1}}{2d_-}\left(1 - \sqrt{1 + \frac{4d_-}{1 - z^{-1}}}\right). \tag{4.25}$$

Substituting these into the second equation gives

$$\sqrt{1 + \frac{4d_-}{1 - z^{-1}}} \quad - \quad r\left(1 - \sqrt{1 - \frac{4d_+}{1 - z}}\right) = 0 \tag{4.26}$$

When $r \ll 1$, the asymptotic solution is

$$z = (1 + 4d_-)^{-1} + O(r), \tag{4.27}$$

and so the discretisation is stable for all values of d_-.

When $r \gg 1$, the asymptotic solution is

$$z \approx 1 - \frac{2rd_+}{\sqrt{1 + 4d_-}} + O(r^{-1}), \tag{4.28}$$

and so the coupled discretisation is still unstable for sufficiently large values of r.

The cross-over from stability to instability again occurs when $z=-1$, giving

$$r = \frac{\sqrt{1+2d_-}}{1-\sqrt{1-2d_+}} \tag{4.29}$$

Thus the condition for stability is

$$r < \frac{\sqrt{1+2d_-}}{1-\sqrt{1-2d_+}} \tag{4.30}$$

Comparing this result with the corresponding result for the purely explicit algorithm, it can be seen that the new stability region is greater except when $d_- \ll 1$. This has a physical interpretation; when d_- is not small, the strong implicit coupling of the computational cells for $j \leq 0$ increases the effective thermal capacity of the cells affected in one timestep by the interface heat flux.

Numerical experiments were performed on the same domain and with the same initial and boundary conditions as before, and with $d_- = 4, d_+ = \frac{3}{8}$. The analysis above predicts stability provided $r < 6$, and this is supported by Figure 3 which shows two sets of results with T_j^n plotted every 25 iterations. In a), $r = 5.95$ and the solution is stable with a slowly decaying interface transient, while in b), $r=6.05$ and the solution is clearly unstable.

4.3 An implicit algorithm

We now consider an algorithm which is implicit on each side of the interface, but with explicit updating of the data used for the interface boundary conditions. The implicit numerical algorithm for $j \leq 0$ is again

$$\begin{aligned} \frac{c_-\Delta x_-}{\Delta t}\,(T_j^{n+1} - T_j^n) &= \frac{k_-}{\Delta x_-}(T_{j+1}^{n+1} - 2T_j^{n+1} + T_{j-1}^{n+1}), \quad j<0 \\ \frac{c_-\Delta x_-}{2\Delta t}\,(T_{0-}^{n+1} - T_{0-}^n) &= -q_w - \frac{k_-}{\Delta x_-}(T_{0-}^{n+1} - T_{-1}^{n+1}). \end{aligned} \tag{4.31}$$

with q_w defined explicitly by

$$q_w = -\frac{k_+}{\Delta x_+}(T_1^n - T_{0+}^n). \tag{4.32}$$

An important point in the above equations is the distinction between T_{0-}^n, the value of T^n at $j=0$ as calculated for the domain $j \leq 0$, and T_{0+}^n, the value of T^n at $j=0$ for the domain $j \geq 0$. In the previous discretisations these two values have been identical but this will not be true in this case.

The corresponding implicit numerical algorithm for simultaneously determining T_j^{n+1} for $j>0$ is

$$\frac{c_+\Delta x_+}{\Delta t}\,(T_j^{n+1} - T_j^n) = \frac{k_+}{\Delta x_+}(T_{j+1}^{n+1} - 2T_j^{n+1} + T_{j-1}^{n+1}). \tag{4.33}$$

The equation for $j=1$ requires the variable T_{0+}^{n+1} and this is set by the Dirichlet boundary condition

$$T_{0+}^{n+1} = T_w, \tag{4.34}$$

where T_w is the interface temperature. Using explicit updating of boundary data,

$$T_w = T_{0-}^n, \tag{4.35}$$

sp T_{0+} lags T_{0-} by one iteration.

The pattern of communication between the calculations for $j \le 0$ and $j \ge 0$ is exactly the same as for the explicit algorithm. They exchange the values of T_w and q_w at the beginning of the timestep, perform the timestep calculations independently (possibly in parallel on separate workstations) and then repeat the process for the next timestep.

For the purposes of analysis it is again more convenient to consolidate and simplify the equations into the following form,

$$\begin{aligned}
T_j^{n+1} &= T_j^n + d_-\left(T_{j+1}^{n+1} - 2T_j^{n+1} + T_{j-1}^{n+1}\right), \qquad j<0 \\
T_{0-}^{n+1} &= T_{0-}^n - 2d_-\left(T_{0-}^{n+1} - T_{-1}^{n+1}\right) + 2rd_+\left(T_1^n - T_{0+}^n\right), \\
T_j^{n+1} &= T_j^n + d_+\left(T_{j+1}^{n+1} - 2T_j^{n+1} + T_{j-1}^{n+1}\right), \qquad j>0 \\
T_{0+}^{n+1} &= T_{0-}^n.
\end{aligned} \tag{4.36}$$

The form of the normal mode solution for this case is

$$T_j^n = \begin{cases} z^n \kappa_-^j, & j = 0-, -1, -2, -3, \dots \\ z^{n-1}\kappa_+^j, & j = 0+,\ 1,\ 2,\ 3, \dots \end{cases}. \tag{4.37}$$

The fourth equation in Equation (4.36) is automatically satisfied by the above choice of normal mode. The other three equations require that the variables z, κ_-, κ_+ satisfy the following equations.

$$\begin{aligned}
1 &= z^{-1} + d_-(\kappa_- - 2 + \kappa_-^{-1}) \\
1 &= z^{-1} + 2d_-(\kappa_-^{-1} - 1) + 2rd_+z^{-2}(\kappa_+ - 1) \\
1 &= z^{-1} + d_+(\kappa_+ - 2 + \kappa_+^{-1})
\end{aligned} \tag{4.38}$$

Solution of the first and third of these equations, subject to the far-field boundary conditions, gives

$$\begin{aligned}
\kappa_-^{-1} &= 1 + \frac{1-z^{-1}}{2d_-}\left(1 - \sqrt{1 + \frac{4d_-}{1-z^{-1}}}\right), \\
\kappa_+ &= 1 + \frac{1-z^{-1}}{2d_+}\left(1 - \sqrt{1 + \frac{4d_+}{1-z^{-1}}}\right).
\end{aligned} \tag{4.39}$$

Substituting these into the second equation gives

$$\sqrt{1+\frac{4d_-}{1-z^{-1}}} \quad + \quad rz^{-2}\left(\sqrt{1+\frac{4d_+}{1-z^{-1}}}-1\right)=0. \tag{4.40}$$

When $r \ll 1$, the asymptotic solution is

$$z=(1+4d_-)^{-1}+O(r), \tag{4.41}$$

and so the discretisation is stable for all values of d_-.

When $r \gg 1$, the asymptotic solution is

$$z \approx \pm i\sqrt{r}\left(\frac{\sqrt{1+4d_+}-1}{\sqrt{1+4d_-}}\right)^{\frac{1}{2}}+O(1). \tag{4.42}$$

Thus for fixed d_-, d_+ and sufficiently large r, the coupled system is unstable.

It is not possible for general values of d_-, d_+ to determine explicitly the value of r above which the solution procedure is unstable. It is possible however to obtain an asymptotic solution under the assumption $d_-, d_+ \gg 1$. This is a reasonable assumption since the motivation in using implicit methods is to use much larger timesteps than would be stable using explicit methods. Under the assumption $d_-, d_+ \gg 1$, Equation (4.40) reduces to

$$\sqrt{d_-} \quad + \quad rz^{-2}\sqrt{d_+} \approx 0, \qquad \Longrightarrow \qquad z \approx \pm i\sqrt{r}\left(\frac{d_+}{d_-}\right)^{\frac{1}{4}}. \tag{4.43}$$

Hence, under these conditions the approximate stability limit is

$$r < \sqrt{\frac{d_-}{d_+}}, \tag{4.44}$$

which can also be re-expressed as

$$\frac{c_+^3 \Delta x_+^4}{k_+} < \frac{c_-^3 \Delta x_-^4}{k_-}. \tag{4.45}$$

Provided, as before, that the correct choice is made as to which domain uses the Neumann b.c.'s and which uses the Dirichlet b.c.'s, then r should be sufficiently small that practical computations will be stable.

Numerical experiments were performed on the same domain and with the same initial and boundary conditions as before, and with $d_- = d_+ = 50$. The approximate stability limit for these values is $r < 1$, and this is supported by Figure 4 which shows two sets of results with T_j^n plotted every 25 iterations. In a), $r = 1.$ and the solution is stable with a slowly decaying interface transient, while in b), $r = 1.1$ and the solution is clearly unstable.

5 Concluding remarks

The stability analysis in this paper has shown the viability of a loosely-coupled approach to computing the temperature and heat flux in coupled fluid/structure interactions. The key point to achieving numerical stability is the use of Neumann boundary conditions for the structural calculation and Dirichlet boundary conditions for the fluid calculation.

Although the analysis was performed here for the 1D model diffusion equation, the results are believed to be applicable to the real situation in which the 3D diffusion equation is used to model the heat flux in the structure and the 3D Navier-Stokes equations are used to model the behaviour of the fluid. This is supported by the practical experience of 3D computations performed using this coupling procedure [1, 4].

The analysis also assumed a time-accurate modelling of the fluid/structure interaction. In practical computations, the point of engineering interest is often the steady-state temperature and heat flux distributions. In such cases, the computations in the structure and fluid can both proceed with different timesteps given by their respective Fourier stability limits. The coupled normal mode analyses remain valid using the values of d_-, d_+ based on the timesteps $\Delta t_-, \Delta t_+$ used in the two domains.

Acknowledgements

This research was supported by Rolls-Royce plc and has benefitted from discussions with Dr. Peter Stow of Rolls-Royce plc and Dr. Mehmet Imregun of Imperial College.

References

[1] R.S. Amano, K.D. Wang, and V. Pavelic. A study of rotor cavities and heat transfer in a cooling process in a gas turbine. *Journal of Turbomachinery*, 116:333–338, 1994.

[2] D. Bohn, G. Lang, H. Schönenborn, and B. Bonhoff. Determination of thermal stress and strain based on a combined aerodynamic and thermal analysis for a turbine nozzle guide vane. ASME Paper 95-CTP-89, 1995.

[3] D. Bohn, H. Schönenborn, B. Bonhoff, and H. Wilhelmi. Prediction of the film-cooling effectiveness in gas turbine blades using a numerical model for the coupled simulation of fluid flow and diabatic walls. ISABE Conference Paper 95-7105, 1995.

[4] J. Chew, I.J. Taylor, and J.J. Bonsell. CFD developments for turbine blade heat transfer. In *3rd International Conference on Reciprocating Engines and Gas Turbines, I. Mech E., London*, number C499-035, 1994.

[5] J. Crank. *The Mathematics of Diffusion.* Clarendon Press, 2nd edition, 1975.

[6] S.K. Godunov and V.S. Ryabenkii. *The Theory of Difference Schemes–An Introduction.* North Holland, Amsterdam, 1964.

[7] A. Heselhaus and D.T. Vogel. Numerical simulation of turbine blade cooling with respect to blade heat condution and inlet temperature profiles. AIAA Paper 95-3041, 1995.

[8] A. Heselhaus, D.T. Vogel, and H. Krain. Coupling of 3D Navier-Stokes external flow calculations and internal 3D heat conduction calculations for cooled turbine blades. In *AGARD CP-527, Heat Transfer and Cooling in Gas Turbines*, 1992.

[9] J. Moore, J. G. Moore, G. S. Henry, and U. Chaudry. Flow and heat transfer in turbine tip gaps. *Journal of Turbomachinery*, 111:301–309, July 1989.

[10] K.W. Morton and D.F. Mayers. *Numerical Solution of Partial Differential Equations – an Introduction.* Cambridge University Press, Cambridge, 1994.

[11] R.D. Richtmyer and K.W. Morton. *Difference Methods for Initial-Value Problems.* Wiley-Interscience, 2nd edition, 1967. Reprint edn (1994) Krieger Publishing Company, Malabar.

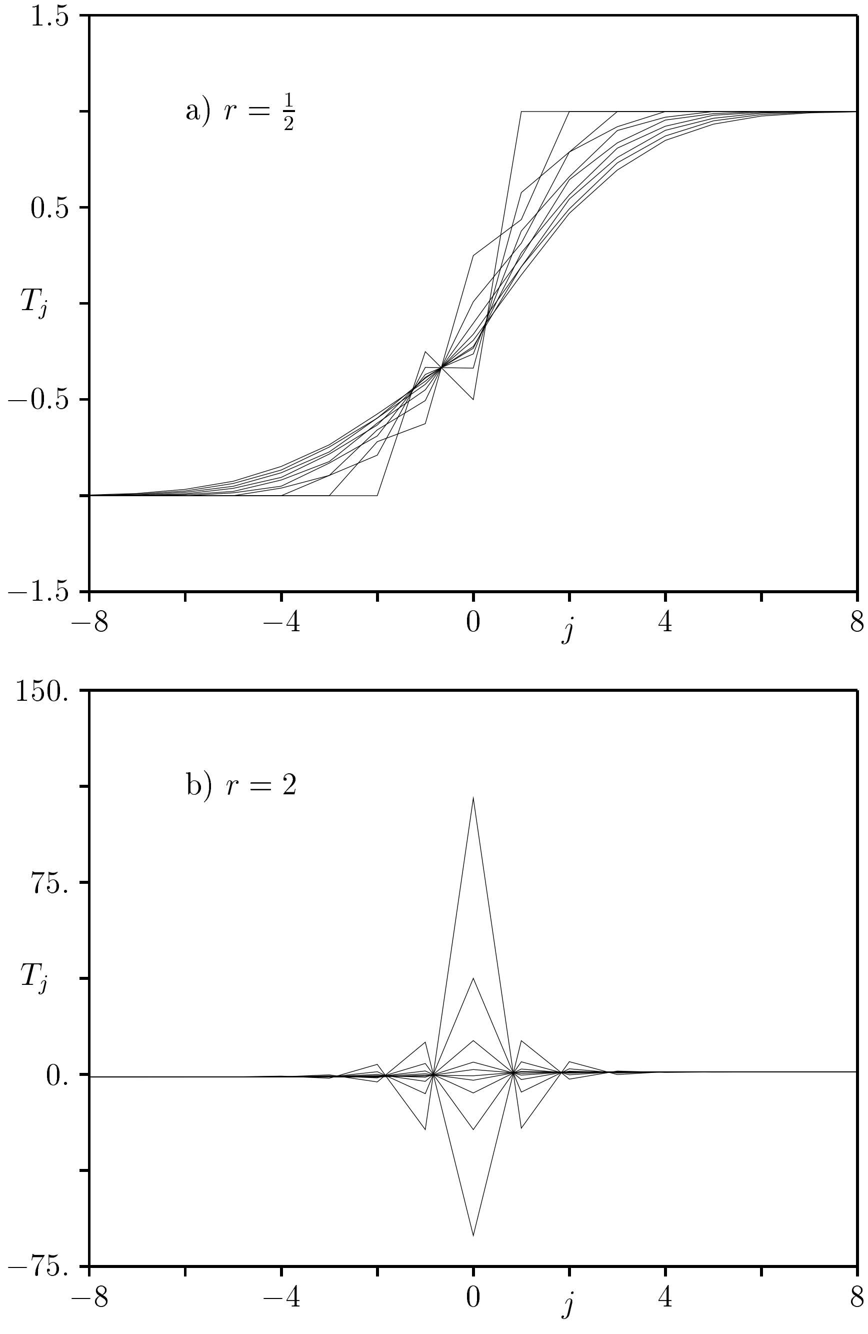

Figure 1: Explicit algorithm with results every iteration

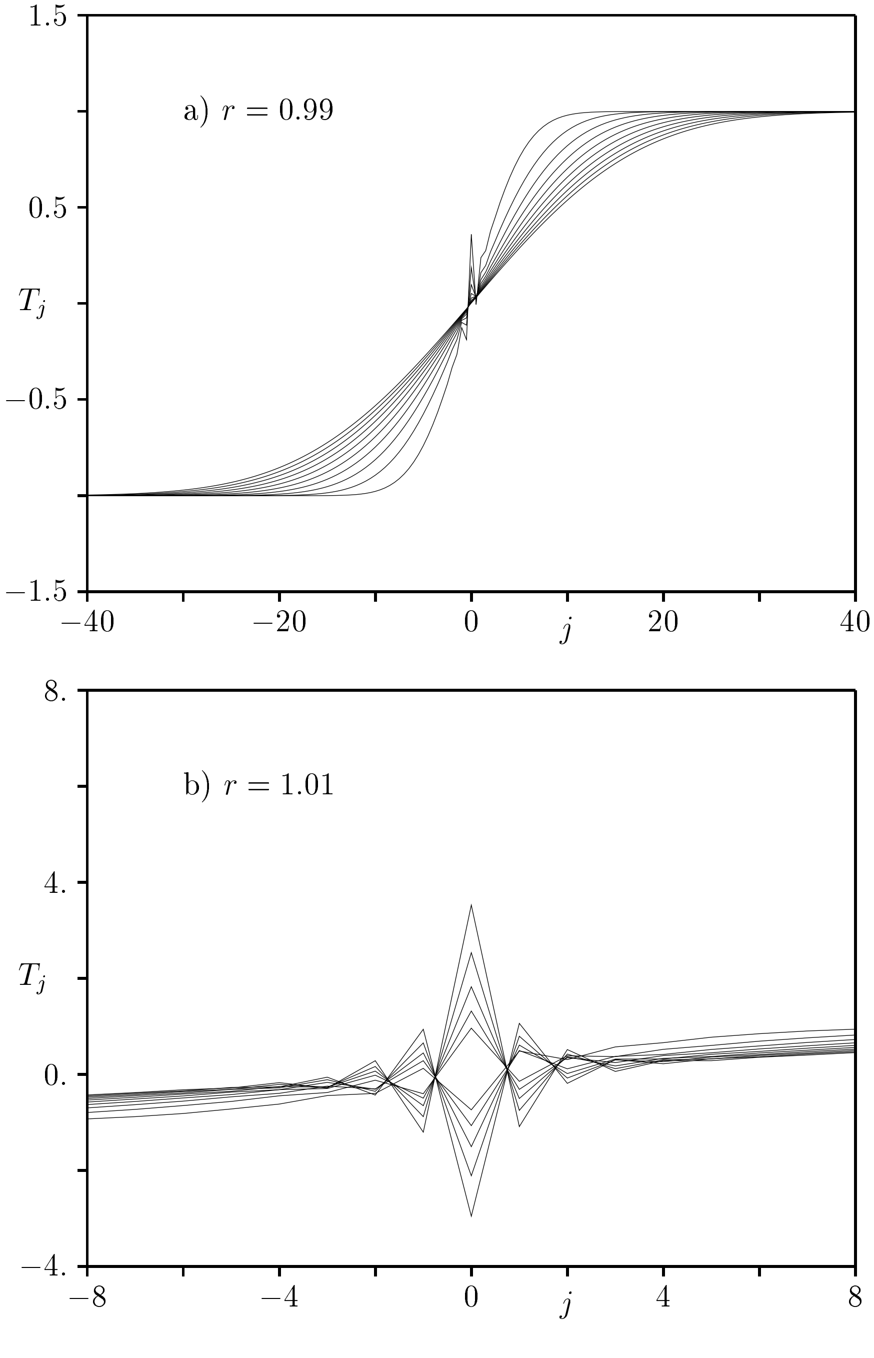

Figure 2: Explicit algorithm with results every 25 iterations

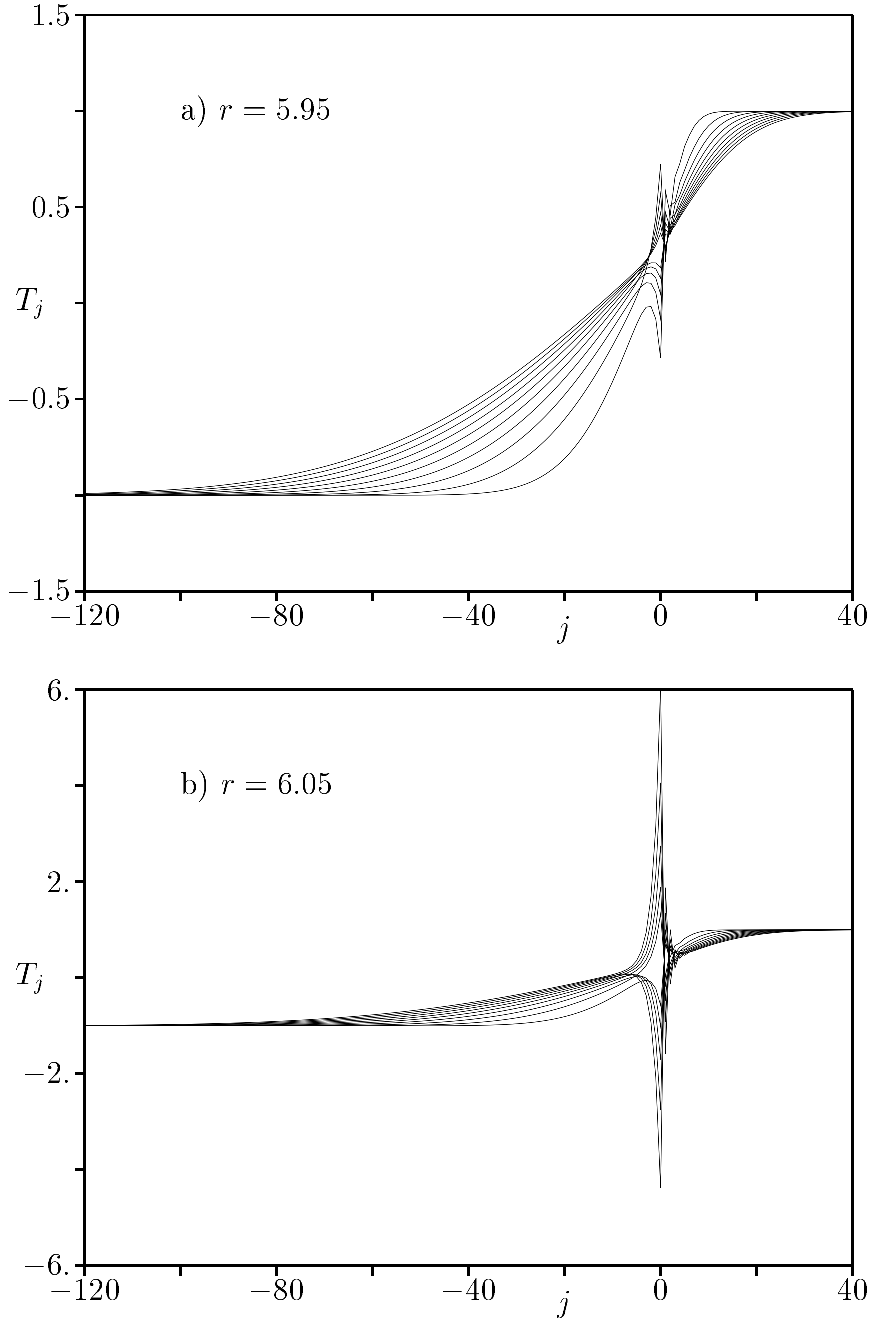

Figure 3: Hybrid algorithm with results every 25 iterations

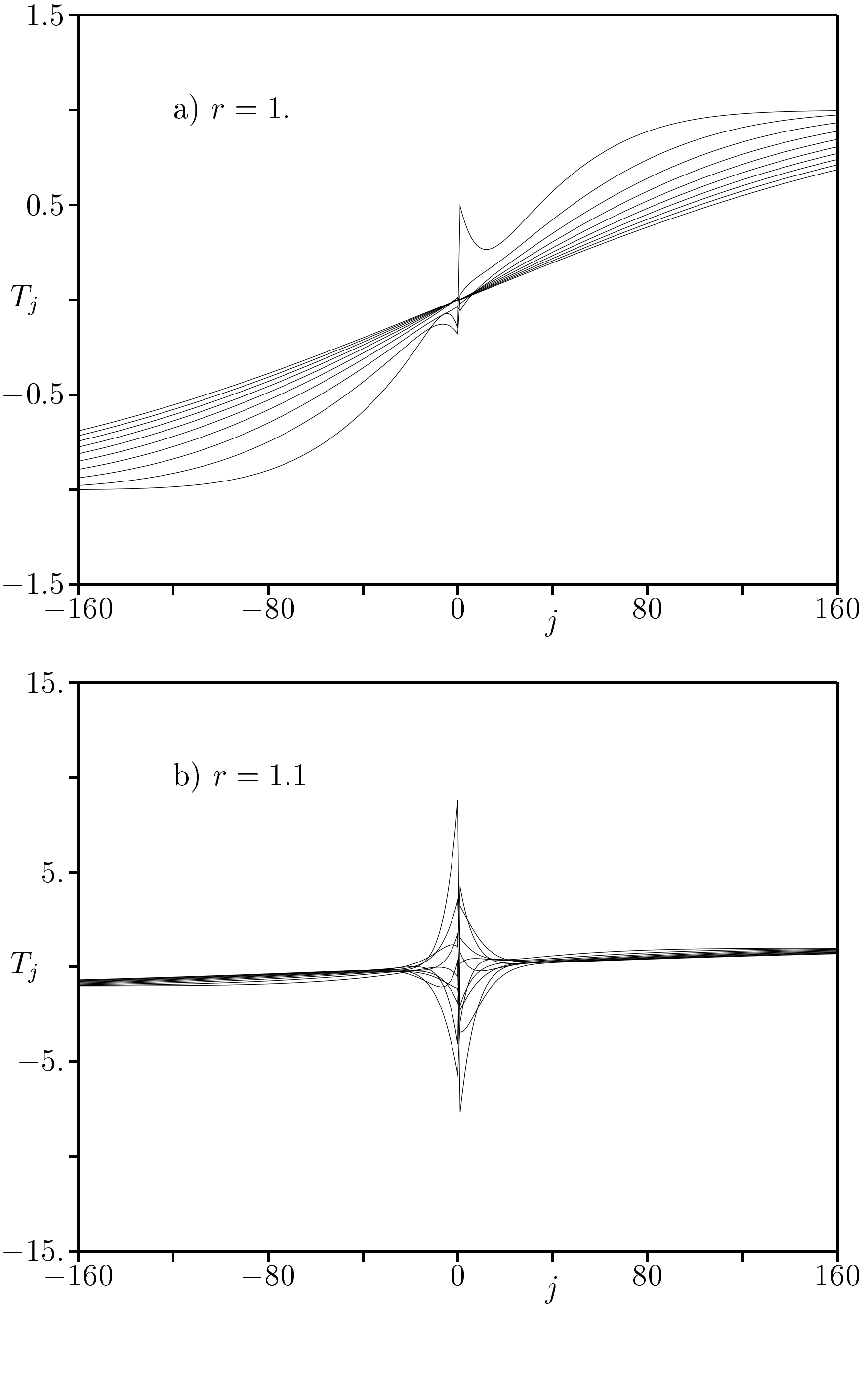

Figure 4: Implicit algorithm with results every 25 iterations